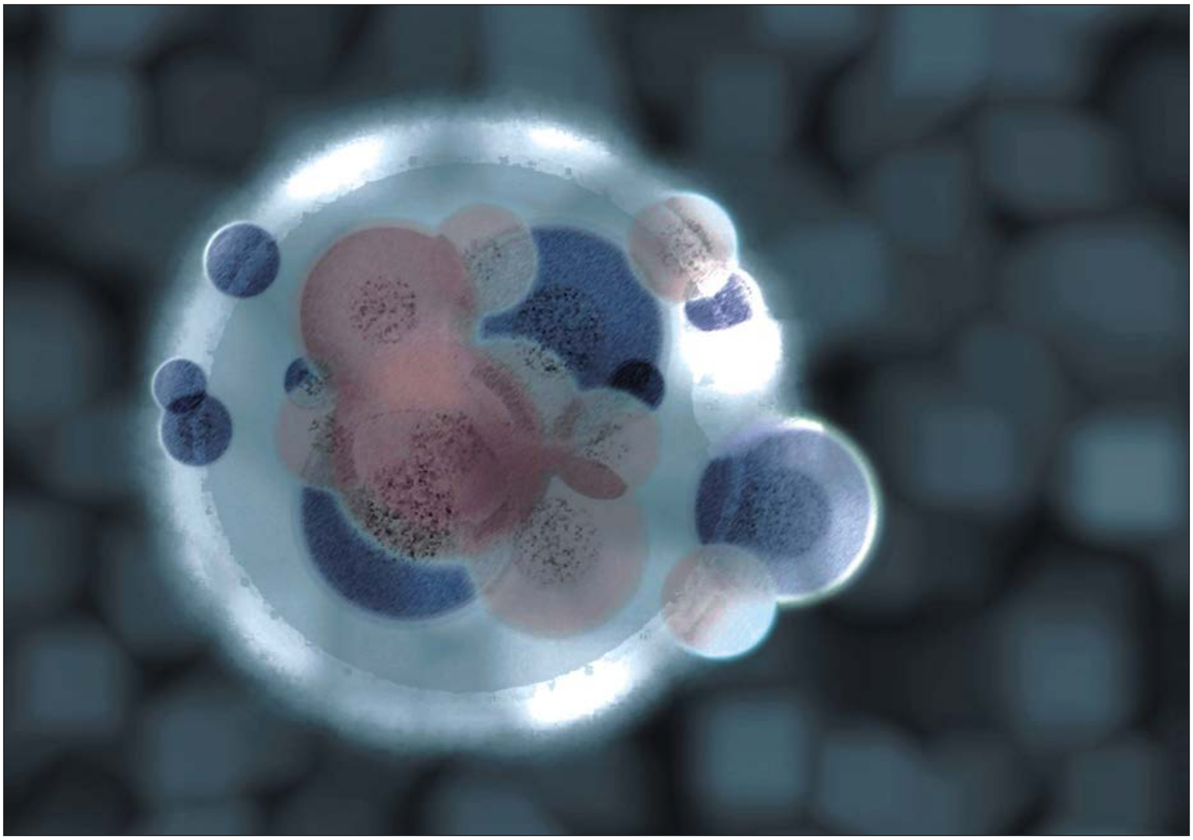

Journal of Biological Sciences

ISSN 1727-3048

science alert

ANSInet
an open access publisher
http://ansinet.com

Journal of Biological Sciences 5 (6): 744-758, 2005
ISSN 1727-3048

Modulation of Dissociation Kinetics by External Force: Examination of the Bell Model

Valentine I. Vullev
Photonics Center, Boston University, 8 St. Mary's Street, Boston, MA 02215, USA

Abstract: Force techniques have been extensively used for studying interactions between macromolecules of biological importance. Bell model, which shows the force influence on the dissociation rates, $\ln(k(F))=\ln(k^{(0)})+\gamma F(k_BT)^{-1}$, has been broadly employed for analysis of force-modulated kinetics. This linear relationship, however, is an approximation. Herein, the conditions for applicability of the Bell model were examined for dissociation processes that proceed through no more than one transition state. The findings show that: (1) the slopes and the intercepts obtained from the linear analyses depend on the force ranges within which the curve fittings are performed; (2) broadening of the force range of analysis compromises the linear approximation provided by Bell model; (3) linear analysis tends to over estimate the values of the dissociation rate constants at zero force, $k^{(0)}$ and (4) limiting the linear analysis to relatively weak forces produces values for $k^{(0)}$ that were close to the expected real values of the rate constant. An alternative interpretation of the slopes and the intercepts obtained from the linear analyses is described. The parameter γ was ascribed to the average separation between the associated and transition states along the reaction pathway within the force range of the linear analysis. The latter was contrary to the broadly accepted view that γ represents the distance between the associated and transition states in the absence of external force. In addition, rather than assigning them to the zero-force activation energy, the intercepts obtained from the linear fits were ascribed to the coordinate-average energies that are differences in the potential energy along the trajectory of dissociation in the absence of external force. These alternative assignments of the linear parameters can prove useful in applications of Bell model for mapping trajectories and landscapes of dissociation processes.

Key words: Force, rate, kinetics, dissociation, trajectory, landscape, pathway, enzyme, inhibitor, potential energy, bound state, transition state, Lennard-Jones

INTRODUCTION

This study discusses the expected changes in dissociation kinetics observed in the presence of external forces. Gaining an understanding of the force dependence of the dissociation rates is essential for quantitative treatment of data obtained from force-measurement techniques such as atomic force microscopy[1-8], dynamic force spectrometry[9-11], laminar-flow force technique[12,13], optical tweezers[7,8,14-16] and magnetic tweezers[17-22]. Employment of force techniques for studying dissociation kinetics has proven very useful not only for estimation of rate constants[23,24], but also for determination of the potential-energy landscapes and trajectories of dissociation[25,26]. Force measurements provide the only approach for obtaining direct experimental information for the latter.

Numerous force-measurement techniques have been utilized for studying various macromolecular multicomponent systems with biological and medical relevance[23,27,28]. About 25 years ago, G. Bell developed a theoretical model for disjointing of cells in the presence of external force[29]. Consequently, his model was readily used for analysis of results from single-molecule force-induced dissociation studies[24,25,30-34]. Using the Kramers' theory[35]. Evans developed a model for force-modulated dissociation on a single-molecule level, interpreting experimental results obtained from systems with complex reaction trajectories, e.g. multiple transition states and under dynamic conditions[10,36,37]. Some of the phenomenological shortcomings of Bell model, i.e. lack of consideration for fluctuations in reaction coordinates, have been addressed and overcome with alternative microscopic treatments[38].

The premise of the Bell model can be stated in the following manner: when a complex is dissociated in the presence of constant external force, F, pointing along the direction of disjoining and the two components are pulled at a distance r from each other (Schemes 1 and 2), the energies of the states of the system will be altered with rF[39].

(In this type of analysis, the distance, r, between the dissociating components is used for a generalized reaction coordinate. Although the force and the reaction coordinate are vector quantities, only their magnitudes are considered because the two vectors are practically parallel: i.e. $\vec{r}\cdot\vec{F} = r\,F\cos\theta \approx rF$. Where, θ is the angle

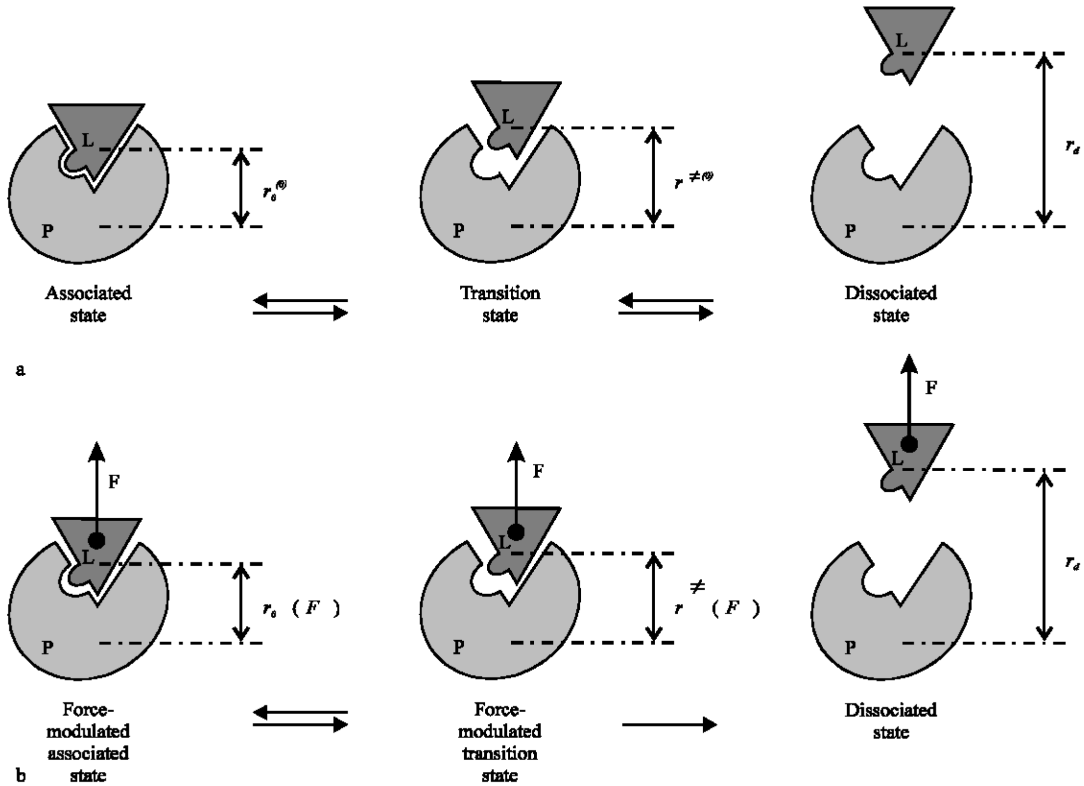

Scheme 1: Dissociation/association process, proceeding through a single transition state, of a complex between a protein, P, and a ligand, L: (a) spontaneous and (b) under the influence of external pulling force

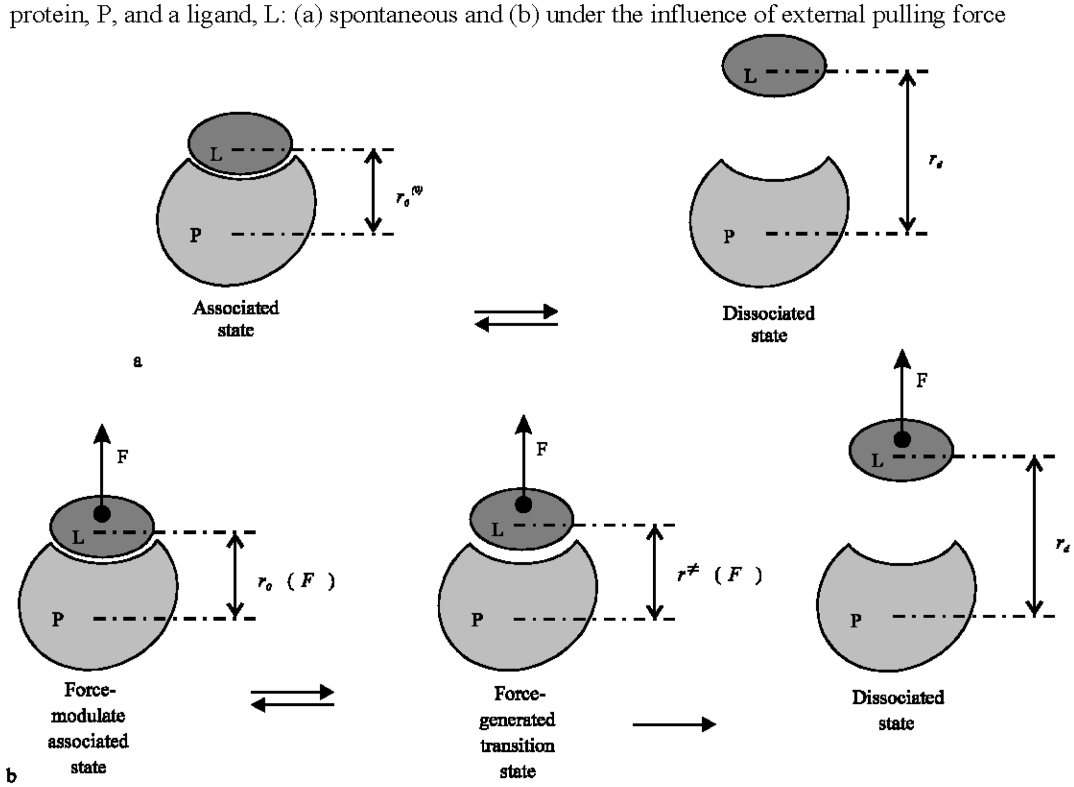

Scheme 2: Dissociation/association process, without a transition state at zero force, of a complex between a protein, P, and a ligand, L: (a) spontaneous and (b) under the influence of external pulling force

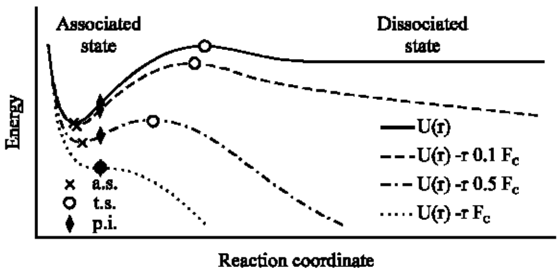

Fig. 1: Changes of the trajectory of an association/dissociation process in the presence of external force, which is pulling the associated species away from each other. U(r) is the potential energy, r is the reaction coordinate and F_C is the critical force at which the dissociation becomes activationless. (a.s. = associated state; t.s. = transition state and p.i. = point of inflection)

between the two vectors and the force has positive values when it is pulling the dissociating species away from each other.) In other words, for a dissociation process whose trajectory is described by a potential energy function U(r), application of external force will change the potential energy to U(r, F), which is linearly dependent on U(r), F and r (Fig. 1)[40].

$$U(r,F) = U(r) - rF \qquad (1a)$$

Application of sufficient external force causes the rate of association to drop to zero, hence, under such conditions only stochastic dissociation events will be observed (Fig.1).

Hence, the activation energy of dissociation in the presence of external force, $E_a(F)$, can be readily estimated from the difference between the energies of the transition state and the associated state, $E^{\neq}$ and E_0, respectively:

$$E_a(F) = E^{\neq}(F) - E_0(F) = U(r^{\neq}) - U(r_0) - (r^{\neq} - r_0)F \qquad (1b)$$

An assumption that the reaction coordinates of the associated and the transition state, r_0 and $r^{\neq}$, respectively, do not depend on the external force, F, yields the following linear expression:

$$E_a(F) = \ni_a^{(0)} - \gamma F \qquad (1c)$$

where, according to Bell, $\ni_a^{(0)}$ is the activation energy in the absence of force[41] and γ is an empirical parameter with dimensions of distance along the reaction coordinates.

(The superscript (0) designates quantities in the absence of external force, i.e. at F = 0.)

Therefore, Eq. (1c) indicates that the logarithmic value of the rate constant of dissociation is linearly proportional to the magnitude of the external force:

$$k_d(F) = A\exp\left(-\frac{E_a(F)}{k_B T}\right) = \kappa_d^{(0)}\exp\left(\frac{\gamma}{k_B T}F\right) \qquad (2a)$$

$$\ln\left(k_d(F)\right) = \mathrm{In}(\kappa_d^{(0)}) + \frac{\gamma}{k_B T}F \qquad (2b)$$

where A is the Arrhenius pre-exponential factor, k_B is the Boltzmann constant, T is the absolute temperature and $\kappa_d^{(0)}$ is the expected dissociation rate constant in the absence of external force based on Eq. 1c, i.e. $\kappa_d^{(0)} = A\exp(-\ni_a^{(0)} / k_B T)$[41].

(The superscript (0) designates quantities in the absence of external force, i.e. at F = 0.)

A principal shortcoming of Bell model, however, is the assumption that the reaction coordinates of the transition and the associated state, $r^{\neq}$ and r_0, respectively, remain constant in the presence of external force, Eq. (1b). As shown in Fig .1, the increase in the applied force shifts the associated and the transition state towards each other until they merge and the dissociation process becomes activationless.

Although a few theoretical frameworks that demonstrate a nonlinear force dependence of $\ln(k_d(F))$ on F have been developed[27,39,40], linear approaches based on Bell model have been broadly used for the analysis of results from force-measurement experiments[4,6,12,19,38,44-46]. It appears that the nonlinearity in the dependence of $\ln(k_d(F))$ on force can be viewed as a perturbation term added to the linear model Eq. 2b. There has not been a clear distinction of the limits within which this perturbation can be ignored without significant consequences for the analyses of force modulated measurements.

The parameter γ has been ascribed to the distance between the associated and the transition state in the absence of external force[4,6,24,32,33,38,44,46]. Apparently, such an assignment for γ is an approximation because r_0 and $r^{\neq}$ are force dependent. The non-linearity in the dependence of $\ln(k_d(F))$ on F, therefore, is expected to affect not only this approximation for γ, but also the estimation of the values of the activation energy and the rate constant at zero force.

This publication offers an analysis of dissociation kinetics in the presence of external force. The basic expressions for a force-modulated dissociation process with no intermediates, i.e. one or no transition state in the absence of force, are shown. No limitations have been imposed on the shape of the potential energy function, U(r), which describes the process of the dissociation. These expressions were applied to two models for U(r), with and without a transition state. A classical Lennard-Jones potential energy function was used for illustration of processes with no transition state[44], while for processes with a single transition state, a composed-parabolic potential energy model was developed. The nonlinear dependence of the activation energy on the applied force is demonstrated.

Linear least-square fits were employed for examination of the feasibility of the Bell model in various regions of forces with different magnitudes. The findings reveal that application of Bell model to data collected in the presence of narrow range of relatively weak external forces yields values of $\ni_a^{(0)}$ and $\kappa_d^{(0)}$ that are close to the real values of the zero-force activation energy and rate constant, respectively. The values obtained for γ even at relatively weak forces, however, do not always represent the conventionally accepted zero-force characteristics of the reaction trajectories. In particular, assignment of γ to a zero-force reaction-coordinate difference between an associated and a transition state is meaningless for dissociation processes with no transition state in the absence of force. Alternative interpretations for the parameters γ and $\ni_a^{(0)}$, that do not limit the linear analyses to only relatively weak forces, were discussed.

MATERIALS AND METHODS

General considerations: This study concentrates on the determination of the dependence of the activation energy, E_a, on the applied external force. The results obtained for $E_a(F)$ were to be readily applied to the dissociation rate constants, Eq. 2a. The force dependent activation energy, $E_a(F)$, for a dissociation process was, in general, calculated by sequential determination of: (1) the reaction coordinates of the associated and the transition state, $r_0(F)$ and $r^‡(F)$, respectively, in the presence of external force; (2) the energies of the associated and the transition state, $E_0(F)$ and $E^‡(F)$, respectively, in the presence of external force and (3) the difference between the two energies, i.e. $E_a(F) = E^‡(F)-E_0(F)$, Eq. (1b). Alternatively, $E_a(F)$ can be directly evaluated from an analytical expression for the activation energy as a function of force should such an expression is available.

Equation 1a shows that in the presence of external force, the reaction coordinates of the associated and the transition state, $r_0(F)$ and $r^‡(F)$, respectively, can be readily evaluated from the first derivative of the potential energy, U(r), that represents the dissociation trajectory in the absence of external force (i.e. from $dU(r,F)/dr = 0$):

$$\frac{dU(r)}{dr} = F \tag{3}$$

The solution of Eq. 3 that corresponds to $r_0(F)$ satisfies $d^2U(r)/dr^2\,|_{r=r^‡} > 0$ and the solution that corresponds to $r^‡(F)$ satisfies $d^2U(r)/dr^2\,|_{r=r^‡} < 0$. When the first derivative of U(r) results in an expression that does not allow analytical solutions for Eq. 3, the values of $r_0(F)$ and $r^‡(F)$ are calculated numerically.

The force-modulated activation energy is calculated from the solutions of Eq. 3 and the zero-force potential energy, U(r), of the process:

$$E_0(F) = U(r_0(F))-F\, r_0(F) \tag{4a}$$

$$E^‡(F) = U(r^‡(F))-F\, r^‡(F) \tag{4b}$$

$$E_a(F) = E^‡(F)-E_0(F) \tag{4c}$$

Alternatively, the force-dependent separation between the associated and the transition state, $\Delta r(F)$, can also be utilized for calculation of $E_a(F)$:

$$\Delta U(F) = U(r^‡(F))-U(r_0(F)) \tag{5a}$$

$$\Delta r(F) = r^‡(F)-r_0(F) \tag{5b}$$

$$E_a(F) = \Delta U(F)-F\, \Delta r(F) \tag{5c}$$

A direct relationship between $\Delta r(F)$ and $E_a(F)$ is readily obtained from Eq. 3 and 5:

$$\Delta r(F) = -\frac{dE_a(F)}{dF} \tag{6}$$

The point of inflection of U(r) is where the concavity of the potential-energy curve changes. It occurs at coordinate r_I and is the point at which the second derivative of U(r, F) becomes zero. Because d^2U/dr^2 does not depend on F, r_I is invariant to external forces (Fig. 1). (Only the point of inflection, r_I, that is situated between the transition and the associated state is of interest to this analysis). Importantly, r_I is the merging point for $r_0(F)$ and $r^‡(F)$, i.e. increase in the external force causes $r_0(F)$ to increase towards r_I and $r^‡(F)$ to decrease towards r_I. When the external pulling force reaches a critical magnitude, F_C, the activation barrier of dissociation is depleted, i.e. $E_a(F)_{F \geq F_C}$ and $E_a(F)_{F<F_C} > 0$. Because $r_0(F_C) = r^‡(F_C) = r_I$, the critical force can be calculated from the first derivative of U(r), Eq. 3:

$$F_c = \left(\frac{dU(r)}{dr}\right)_{r=r_I} \qquad (7)$$

The analysis, presented in this study, concentrates on the range of forces between 0 and F_C.

Models for U(r): Analyses in this study are based on two models for potential-energy landscapes for association-dissociation processes, described by composed-parabolic (or parabolic-parabolic, PP) and Lennard-Jones (LJ) potential energy functions.

Composed-parabolic model: The composed parabolic potential function, $U_{PP}(r)$, comprises one convex and one concave parabola, which are smoothly connected at the point of inflection, r_I:

$$U_{PP}(r) = \begin{cases} U_{P1}(r) & \text{if } r \le r_I \\ U_{P2}(r) & \text{if } r > r_I \end{cases} \qquad (8)$$

where,

$$U_{P1}(r) = \frac{\kappa}{n}\left|r - r_0^{(0)}\right|^n + E_0^{(0)} \text{ and } U_{P2}(r) = -\frac{\phi}{s}\left|r^{\neq(0)} - r\right|^s + E^{\neq(0)}$$

The composed parabolic function is a good model for a process that proceeds through a single transition state in the absence of external force (Scheme 1). Apparently, $U_{PP}(r)$ depends on the energy and the reaction coordinates of the associated and the transition state, $E_0^{(0)}$, $r_0^{(0)}$, $E^{\neq(0)}$ and $r^{\neq(0)}$, respectively. (The superscript (0) designates quantities in the absence of external force, i.e. at F = 0.) Without compromising the depth of the analysis, the expressions were simplified by using differential quantities for the energy and the reaction coordinates: i.e. $\varepsilon = E_a^{(0)} = E^{\neq(0)} - E_0^{(0)}$; $R = \Delta r^{(0)} = r^{\neq(0)} - r_0^{(0)}$ and the values of the associated-state energy and reaction coordinate at the potential minimum are set to zero: i.e. $E_0^{(0)} = 0$ and $r_0^{(0)} = 0$. The point of inflection of $U_{PP}(r)$ is determined by a parameter q that has a value between 0 and 1: i.e. $r_I = r_0^{(0)} + qR$. The steepness of $U_{P1}(r)$ and $U_{P2}(r)$ depends on the order of the parabolas, n and s, respectively (Fig. 2).

The force constants, κ and ϕ, in Eq. (8) are determined from the requirements for $U_{P1}(r)$ and $U_{P2}(r)$ to have the same values and slopes at the connecting point, r_I: i.e. $U_{P1}(r_I) = U_{P2}(r_I)$ and $U_{P1}(r_I)/dr|_{r=r_I} = U_{P1}(r_I)/dr|_{r=r_I}$ resulting in:

$$\kappa = Aq^{1-n}\,\varepsilon\,R^{-n} \qquad (9a)$$

$$\phi = A(1-q)^{1-s}\,\varepsilon\,R^{-s} \qquad (9b)$$

where, $A = \dfrac{ns}{n - nq + sq}$.

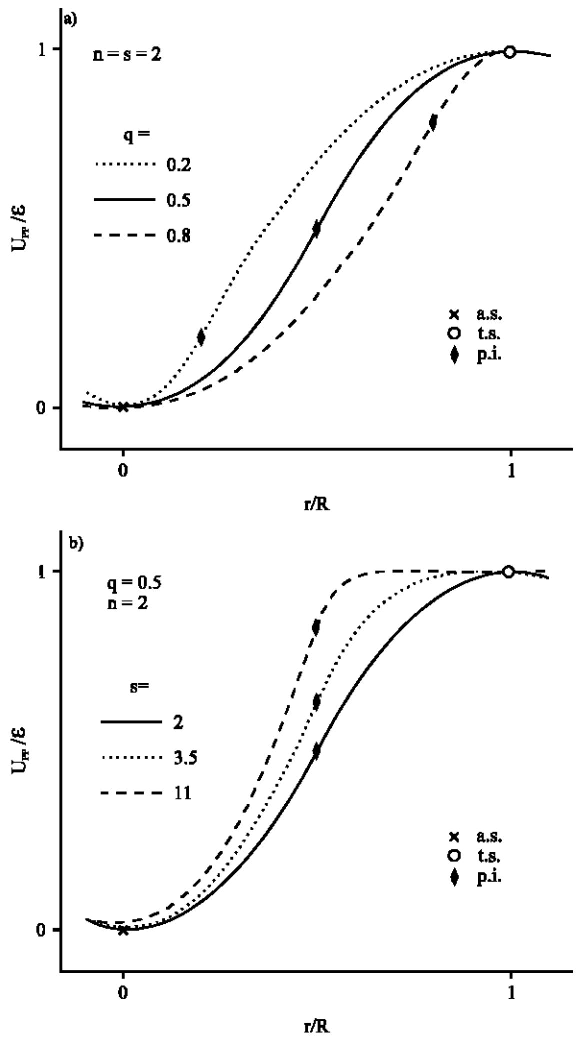

Fig. 2: Reaction pathways described by various composed parabolic potential energy functions, U_{PP}, Eq. 8, for: (a) different values of q when n = s = 2 and (b) different values of s when q = 0.5 and n = 2. The graphs show only the regions between the associated and the transition state that are of interest for this analysis. (a.s. = associated state; t.s. = transition state and p.i. = point of inflection)

The critical force for $U_{PP}(r)$ is obtained from Eq. 7-9:

$$F_C = A\,\varepsilon\,R^{-1} \qquad (10)$$

The solutions of Eq. 3 for $U(r) = U_{PP}(r)$, together with the definition of $U_{PP}(r)$, Eq. 8, yields expressions for the activation energy, $E_a(F)$ and the reaction-coordinate separation between the associated and the transition state, $\Delta r(F)$, in the presence of external force:

$$\Delta r(F) = r^{\neq}(F) - r_0(F) = R - f(F) \qquad (11a)$$

$$E_a(F) = \varepsilon - RF + \alpha_n F^{\frac{n}{n-1}} + \alpha_s F^{\frac{s}{s-1}} \qquad (11b)$$

where, the force-dependent perturbation terms are $f(F) = \left(\frac{F}{\kappa}\right)^{\frac{1}{n-1}} + \left(\frac{F}{\phi}\right)^{\frac{1}{s-1}}$, $\alpha_n F^{\frac{n}{n-1}} = q\frac{n-1}{n} A^{\frac{1}{1-n}} \varepsilon^{\frac{1}{1-n}} R^{\frac{n}{1-n}} F^{\frac{n}{n-1}}$ and $\alpha_s F^{\frac{s}{s-1}} = (1-q)\frac{s-1}{s} A^{\frac{1}{1-s}} \varepsilon^{\frac{1}{1-s}} R^{\frac{s}{1-s}} F^{\frac{s}{s-1}}$. Notice that $dE_a(F)/dF = \Delta r(F)$, Eq. 6.

Lennard-Jones model: Lennard-Jones potential energy function, $U_{LJ}(r)$, is comprised of an attraction and a repulsion components, proportional to r^{-12} and r^{-6}, respectively[44-47].

$$U_{LJ}(r) = 4\varepsilon\left(\left(\frac{\sigma}{r}\right)^{12} - \left(\frac{\sigma}{r}\right)^{6}\right) \qquad (12)$$

where ε is the depth of the potential-energy well of the associated state and corresponds to the activation energy of dissociation and σ determines the width of the well and is equal to the coordinate at which $U_{LJ} = 0$ (Fig. 3). For example, the width of the potential-energy well at half-depth (i.e. at $U_{LJ} = -\varepsilon / 2$) is ~ 0.35σ.

The Lennard-Jones function is a good model for an activationless association processes (Scheme 2). Because the interacting species do not have to surpass any energy barrier in order to reach the associated state, there is no defined transition state in the absence of external force, i.e. U_{LJ} at F = 0 asymptotically approaches zero as r increases to infinity. The zero-force reaction coordinates of the associated state and the point of inflection are determined from the first and second derivatives of U_{LJ}: $r_0^{(0)} = 2^{1/6}\sigma \approx 1.122\sigma$; $r_I = (26/7)^{1/6}\sigma \approx 1.244\sigma$; From $r_{,I}$ the critical force for U_{LJ} is evaluated (Eq. 7):

$$F_c = \frac{252}{169}\sqrt[6]{\frac{2^5 7}{13}}\frac{\varepsilon}{\sigma} \approx 2.3964\frac{\varepsilon}{\sigma} \qquad (13)$$

Application of an external pulling force results in appearance of a transition state on $U_{LJ}(r)$ (Fig. 3). The reaction coordinate of this force-generated transition state, $r^{\neq}(F)$, reflects the point in the reaction pathway at which the external force is balanced by the interaction forces between the dissociating components of the complex (Scheme 2). The reaction coordinates of the associated and the transition state in the presence of force can be obtained from numerical solutions of a polynomial equation that is a combination of Eq. 3 and 12:

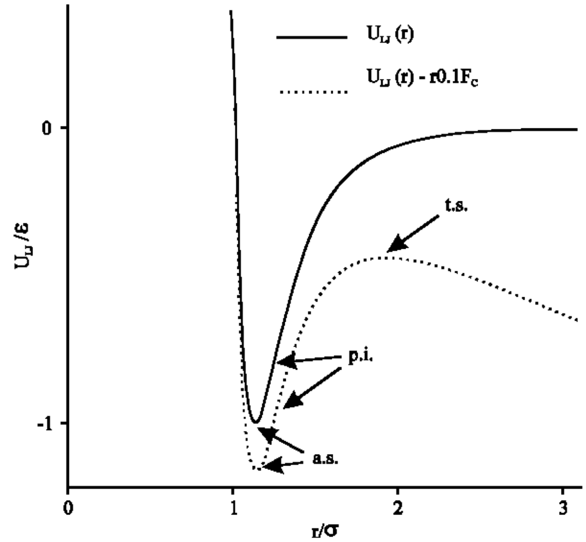

Fig. 3: Lennard-Jones potential energy functions, U_{LJ}, Eq. 12, in the presence and absence of external force. (a.s. = associated state; t.s. = transition state and p.i. = point of inflection)

$$r^{13} - \frac{24\varepsilon\sigma^6}{F} r^6 + \frac{48\varepsilon\sigma^{12}}{F} = 0 \qquad (14)$$

The resultant $r_0(F)$ and $r^{\neq}(F)$ are used for calculation of $E_0(F)$, $E^{\neq}(F)$, $\Delta r(F)$, $\Delta U(F)$ and $E_a(F)$ from Eq. 4 and 5.

Linear analysis based on the Bell model: The curves for $E_a(F)$ vs. F obtained from the composed-parabolic and Lennard-Jones models for U(r), were fit to Eq. (1c) using least-square formalism:

$$\gamma = \frac{n\sum_{i=j}^{v} F_i E_a(F_i) - \sum_{i=j}^{v} F_i \sum_{i=j}^{v} E_a(F_i)}{n\sum_{i=j}^{v} F_i^2 - \left(\sum_{i=j}^{v} F_i\right)^2} \qquad (15a)$$

$$Э_a^{(0)} = \frac{1}{n}\left(\sum_{i=j}^{v} E_a(F_i) - \gamma\sum_{i=j}^{v} F_i\right) \qquad (15b)$$

where, the fits were performed between the points j and v and n is the total number of points within the fitting range, i.e. n = v-j + 1; F_i is the value of the force at point i.

Durbin-Watson criterion (DW) was used for estimation of the quality of the linear fits[48,49].

$$DW = \frac{\sum_{i=j+1}^{v} \left(e_a(F_i) - e_a(F_{i-1})\right)^2}{\sum_{i=j}^{v} \left(e_a(F_i)\right)^2} \qquad (16)$$

where, $e_a(F_i)$ are the residuals from the curve fits, i.e. $e_a(F_i) = E_a(F_i) - Э_a^{(0)} + \gamma F_i$.

Quantities averaged over a force region: For analysis in a region between forces F_j and F_v, the force-average associated-transition state separation $<\Delta r_{jv}>$ along the reaction coordinates, is:

$$< \Delta r_{jv} >= \left(F_v - F_j\right)^{-1} \int_{F_j}^{F_v} \Delta r(F) dF \qquad (17a)$$

Substitution of Eq. (6) in the integral function yields:

$$< \Delta r_{jv} >= \frac{E_a(F_j) - E_a(F_v)}{F_v - F_j} \qquad (17b)$$

The force corresponding to the average associated-transition state separation, F_{jv}, at which $\Delta r(F)$ is equal to the average separation between the associated and the transition state, $<\Delta r_{jv}>$, can be extracted from the following relationship:

$$\Delta r(F_{jv}) = <\Delta r_{jv}> \qquad (18)$$

Substitution of F_{jv} in Eq. (5a) produces the coordinate-average energy, ΔU_{jv}, which is the potential-energy difference between two points on the force-unperturbed U(r). These two points correspond to the reaction coordinates of the associated and the transition state at force F_{jv} (Eq. 5a):

$$\Delta U_{jv} = \Delta U(F_{jv}) = U(r^*(F_{jv}))-U(r_0(F_{jv})) \qquad (19)$$

Computations: All calculations and analyses are performed on Pentium 4 workstation, using macros written for IgorPro software, v. 4 (WaveMetrics, Inc., Lake Oswego, OR 97035, U.S.A.).

For simplicity of the analysis, the quantities used in this publication are unitless: the forces are normalized to F_C (or ε /R and ε /σ for U_{PP} and U_{LJ}, respectively), the energies-to ε and reaction coordinates-to R and σ for U_{PP} and U_{LJ}, respectively.

It should be emphasized that in this study, ε denotes the activation energy in the absence of external force, while $\ni_a^{(0)}$ is the intercept obtained from linear fits of the $E_a(F)$ vs. F curves (Eq. 1c). One of the criteria for the applicability of the Bell model is how close the values of $\ni_a^{(0)}$ and ε are, i.e. ideally, $\ni_a^{(0)}/\varepsilon \to 1$.

RESULTS

For dissociation processes described by the composed-parabolic model (Eq. 8) the force dependence of the activation energy was calculated for 27 combinations of various values of q, n and s (q = 0.2, 0.5, 0.8; n = 2, 3.5, 11 and s = 2, 3.5, 11) that correspond to 12 different curves for E_a vs. F (Fig. 4a). (When n = s, E_a does not depend on q. If $n_i = s_j$ and $n_j = s_i$ and $q_i = 1-q_j$, then $E_{ai}(F) = E_{aj}(F)$.) The exact values for $E_a(F)$ and $\Delta r(F)$ were calculated using the corresponding analytical expressions (Eq. 11). As expected, increase in the applied pulling force lowers the activation energy nonlinearly. The initial decrease in $E_a(F)$ at small values for F/F_C is most profound for n = s = 11 and least acute for n = s = 2. The other ten curves for $E_a(F)$ are situated between the activation-energy curves for n = s = 2 and n = s = 11.

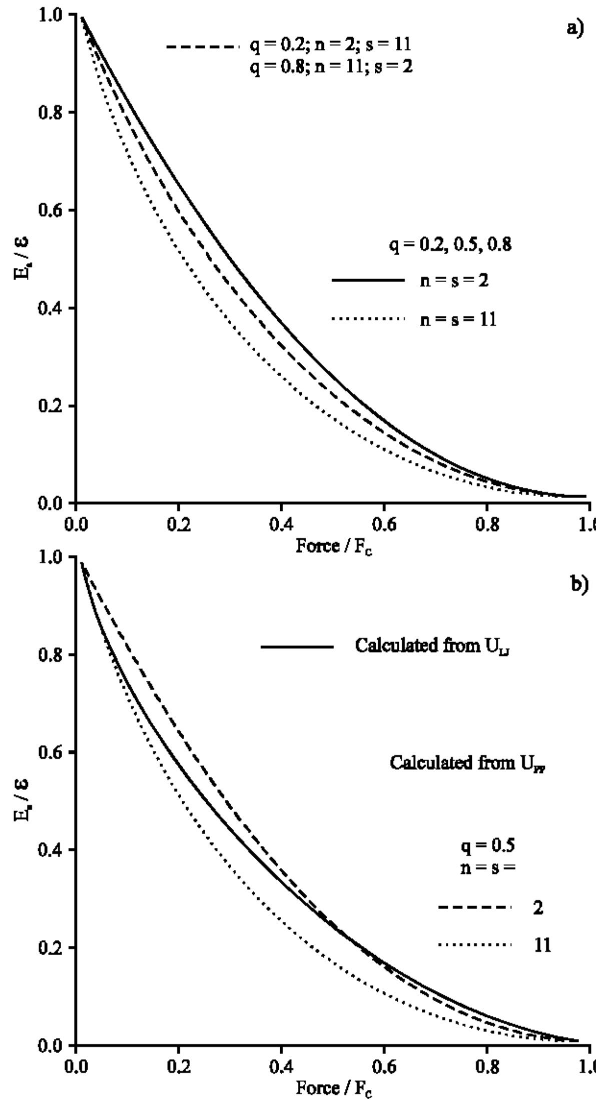

Fig. 4: Dependence of the activation energy of dissociation on the applied force for processes described by: (a) composed parabolic potential energy, U_{PP} (When n = s, E_a does not depend on q. If $n_i = s_j$ and $n_j = s_i$ and $q_i = 1-q_j$, then $E_{ai}(F) = E_{aj}(F)$.) and (b) Lennard-Jones potential energy, U_{LJ}, in comparison with the two extreme curves for U_{PP}

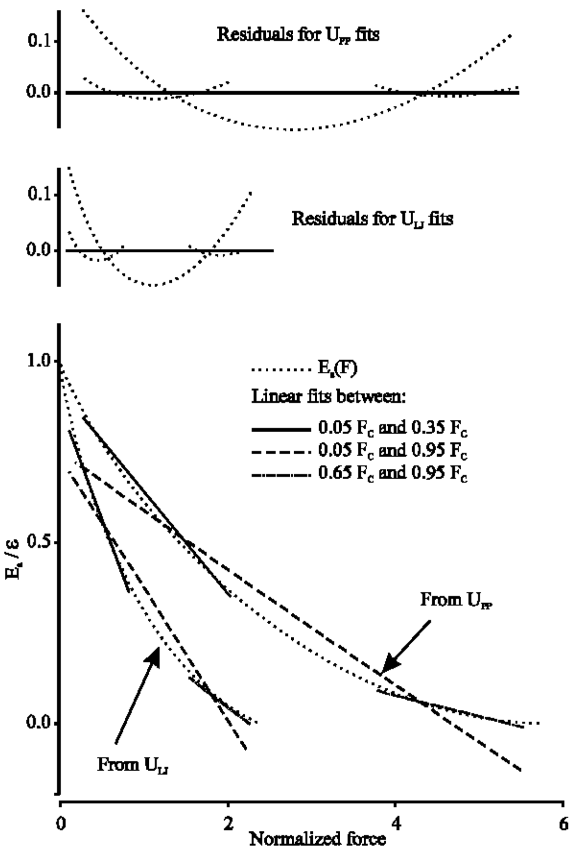

Fig. 5: Examples for linear data fits of $E_a(F)$ vs. F for dissociation processes described by U_{LJ} and U_{PP} (q = 0.2, n = 2, s = 11; or q = 0.8, n = 11, s = 2). (When n = s, E_a does not depend on q. If $n_i = s_j$ and $n_j = s_i$ and $q_i = 1-q_j$, then $E_{a\,i}(F) = E_{a\,j}(F)$.) The fits were performed over various force intervals where, $F_C = 2.496\,\varepsilon/\sigma$ for U_{LJ} and $F_C = 5.79\varepsilon/R$ for U_{PP}. The normalized force is $F/(\varepsilon\,\sigma^{-1})$ for U_{LJ} and $F/(\varepsilon\,R^{-1})$ for U_{PP}

Different regions of the $E_a(F)$ curves were fit to a linear function using Eq. 15a and b (Fig. 5). This analysis is limited to forces between 5% and 95% of the values of F_C. Experimentally, measurements at very weak forces may need to be extended to unfeasibly long time scales. Alternatively, as the force increases towards F_C, the lifetimes of the associated state will decrease below the time resolution of the instruments used for the kinetic measurements. Each of the $E_a(F)$ curves contains one point per $0.01F_C$. The slopes of the fits are equal to the parameters, γ and the intercepts-to $\ni_a^{(0)}$. For each $E_a(F)$ curve, linear fits were performed at six different force regions, limited between F_j and F_v: (1) one broad force region, covering 90% of F_C, spanning from $0.05F_C$ to $0.95F_C$; (2) two medium-wide regions, covering 60% of F_C, from $0.05F_C$ to $0.65F_C$ and from $0.35F_C$ to $0.95F_C$ and (3) three relatively narrow regions, covering 30% of F_C, from $0.05F_C$ to $0.35F_C$, from $0.35F_C$ to $0.65F_C$ and from $0.65F_C$ to $0.95F_C$. Table 1 to 12 summarize the results from the linear fits of E_a vs. F for activation energy curves obtained from the various combinations of n, s and q for a composed-parabolic model.

The same calculations and analysis were performed for a dissociation process with no zero-force transition state that follows the Lennard-Jones potential-energy function (Eq. 12) and the results are shown in Table 13. The force dependent reaction coordinates, $r_0(F)$ and $r^*(F)$, were calculated numerically from Eq. 14 and the resulting values were input in Eq. 5, where $U(r) = U_{LJ}(r)$ (Eq. 12), to obtain $E_a(F)$ and $\Delta r(F)$. In comparison with the curves obtained from the composed-parabolic models, the values of the curve for $E_a(F)$ obtained from the Lennard-Jones potential-energy function decrease faster at relatively weak forces and slower at forces closer to F_C (Fig. 4b). Furthermore, unlike their counterpart curves obtained from U_{PP}, the $\Delta r(F)$ curve calculated from U_{LJ} sharply descends from infinity to about σ in the weak-force range between 0 and $0.05F_C$ (Fig. 6b).

Because the activation-energy curves are obtained from exact calculations and they do not contain any noise or experimental errors, the autocorrelation Durbin-Watson statistics, together with Eq. (1c), provides a good measure for the linearity of the dependence of $E_a(F)$ on F. Should the fitting function (Eq. 1c) is a good model for the force-dependence of the activation energy, the values obtained for DW will be larger than ~ 1.2 for n > ~ 30. The strong autocorrelation due to the nonlinearity in the $E_a(F)$ vs. F relationship, is reflected in the extremely small DW values, shown in the tables.

When the Bell model was applied to the calculated $E_a(F)$ vs. F curves, the residuals indicate that the linear fits improve when limited to short spans of the curves, e.g. $|F_v-F_j|$ is smaller than about 30 % of F_C (Fig. 5). Because of the convex shapes of the $E_a(F)$ curves, the line fits produce intercepts, $\ni_a^{(0)}$, that are smaller than the value for the activation energy in the absence of force, ε (Table 1-13). The underestimation of the zero-force activation energy, ε, becomes more acute as the limits of the curve fitting, F_j and F_v, move towards larger forces. For example, line fits between $F_j = 0.05F_C$ and $F_v = 0.35F_C$ produce values for $E_a^{(0)}$ that range between 86% and 97% of the expected value for the activation energy in absence of force, ε (Table 1-13). When line fitting is performed between $F_j = 0.65F_C$ and $F_v = 0.95F_C$, the intercept can be as low as 23% of the expected value for ε (Table 2).

Further examination of Table 1-12, indicates that for processes proceeding through a single transition state,

Table 1: Results from analysis of the force dependence of the activation energy for a dissociation process following a U_{PP} potential energy curve, n = s = 2, 0 < q < 1, $F_C = 2\varepsilon R^{-1}$. (When n = s, E_a does not depend on q)

F_j / F_C	F_v / F_C	$\exists_a^{(0)}/\varepsilon$	γ /R	DW	$\langle \Delta r_{jv} \rangle$ /R	$F_{jv} / \varepsilon R^{-1}$	$\Delta U_{jv} / \varepsilon$
5	35	0.968	0.800	0.0568	0.800	0.400	0.960
5	65	0.909	0.650	0.0154	0.650	0.700	0.878
5	95	0.819	0.500	0.00701	0.500	1.00	0.750
35	65	0.758	0.500	0.0568	0.500	1.00	0.750
35	95	0.609	0.350	0.0154	0.350	1.30	0.578
65	95	0.368	0.200	0.0568	0.200	1.60	0.360

Table 2: Results from analysis of the force dependence of the activation energy for a dissociation process following a U_{PP} potential energy curve, n = s = 11, 0 < q < 1, $F_C = 11\varepsilon R^{-1}$. (When n = s, E_a does not depend on q.)

F_j / F_C	F_v / F_C	$\exists_a^{(0)}/\varepsilon$	γ /R	DW	$\langle \Delta r_{jv} \rangle$ /R	$F_{jv} / \varepsilon R^{-1}$	$\Delta U_{jv} / \varepsilon$
5	35	0.861	0.154	0.0626	0.157	1.98	0.848
5	65	0.761	0.107	0.0181	0.113	3.32	0.732
5	95	0.658	0.0756	0.00862	0.0827	4.64	0.613
35	65	0.546	0.0678	0.0575	0.0683	5.42	0.541
35	95	0.417	0.0441	0.0158	0.0454	6.91	0.400
65	95	0.226	0.0224	0.0571	0.0226	8.75	0.222

Table 3: Results from analysis of the force dependence of the activation energy for a dissociation process following a U_{PP} potential energy curve, n = s = 3.5, 0 < q < 1, $F_C = 3.5\varepsilon R^{-1}$. (When n = s, E_a does not depend on q.)

F_j / F_C	F_v / F_C	$\exists_a^{(0)}/\varepsilon$	γ /R	DW	$\langle \Delta r_{jv} \rangle$ /R	$F_{jv} / \varepsilon R^{-1}$	$\Delta U_{jv} / \varepsilon$
5	35	0.916	0.483	0.0597	0.488	0.656	0.904
5	65	0.830	0.357	0.0167	0.367	1.12	0.798
5	95	0.729	0.260	0.00775	0.273	1.58	0.673
35	65	0.633	0.244	0.0572	0.245	1.73	0.626
35	95	0.492	0.163	0.0156	0.166	2.22	0.470
65	95	0.278	0.0862	0.0569	0.0867	2.79	0.272

Table 4: Results from analysis of the force dependence of the activation energy for a dissociation process following a U_{PP} potential energy curve, (n = 2 and s = 11) or (n = 11 and s = 2), q = 0.5, $F_C = 3.38\varepsilon R^{-1}$. (If $n_i = s_j$ and $n_j = s_i$ and $q_i = 1-q_j$, then $E_{a\,i}(F) = E_{a\,j}(F)$.)

F_j / F_C	F_v / F_C	$\exists_a^{(0)}/\varepsilon$	γ /R	DW	$\langle \Delta r_{jv} \rangle$ /R	$F_{jv} / \varepsilon R^{-1}$	$\Delta U_{jv} / \varepsilon$
5	35	0.952	0.477	0.0582	0.479	0.656	0.943
5	65	0.886	0.379	0.0158	0.381	1.15	0.856
5	95	0.794	0.288	0.00721	0.291	1.66	0.730
35	65	0.725	0.284	0.0569	0.284	1.69	0.718
35	95	0.579	0.197	0.0154	0.198	2.19	0.550
65	95	0.346	0.111	0.0568	0.111	2.71	0.339

Table 5: Results from analysis of the force dependence of the activation energy for a dissociation process following a U_{PP} potential energy curve, (n = 2 and s = 3.5) or (n = 3.5 and s = 2), q = 0.5, $F_C = 2.55\varepsilon R^{-1}$. (If $n_i = s_j$ and $n_j = s_i$ and $q_i = 1-q_j$, then $E_{a\,i}(F) = E_{a\,j}(F)$.)

F_j / F_C	F_v / F_C	$\exists_a^{(0)}/\varepsilon$	γ /R	DW	$\langle \Delta r_{jv} \rangle$ /R	$F_{jv} / \varepsilon R^{-1}$	$\Delta U_{jv} / \varepsilon$
5	35	0.949	0.641	0.0581	0.644	0.492	0.940
5	65	0.880	0.503	0.0158	0.508	0.857	0.849
5	95	0.786	0.380	0.00725	0.387	1.22	0.723
35	65	0.712	0.371	0.0569	0.372	1.27	0.705
35	95	0.566	0.256	0.0154	0.258	1.64	0.538
65	95	0.334	0.143	0.0569	0.143	2.03	0.328

Table 6: Results from analysis of the force dependence of the activation energy for a dissociation process following a U_{PP} potential energy curve, (n = 3.5 and s = 11) or (n = 11 and s = 3.5), q = 0.5, $F_C = 5.31\varepsilon R^{-1}$. (If $n_i = s_j$ and $n_j = s_i$ and $q_i = 1-q_j$, then $E_{a\,i}(F) = E_{a\,j}(F)$.)

F_j / F_C	F_v / F_C	$\exists_a^{(0)}/\varepsilon$	γ /R	DW	$\langle \Delta r_{jv} \rangle$ /R	$F_{jv} / \varepsilon R^{-1}$	$\Delta U_{jv} / \varepsilon$
5	35	0.903	0.319	0.0605	0.323	0.984	0.891
5	65	0.813	0.232	0.0170	0.240	1.67	0.782
5	95	0.712	0.168	0.00794	0.178	2.35	0.659
35	65	0.612	0.156	0.0572	0.157	2.63	0.605
35	95	0.474	0.104	0.0157	0.106	3.37	0.453
65	95	0.265	0.0543	0.0570	0.0546	4.23	0.260

Table 7: Results from analysis of the force dependence of the activation energy for a dissociation process following a U_{PP} potential energy curve, (n = 2, s = 11 and q = 0.8) or (n = 11, s = 2 and q = 0.2), $F_C = 2.39\varepsilon R^{-1}$. (If $n_i = s_j$ and $n_j = s_i$ and $q_i = 1-q_j$, then $E_{a\,i}(F) = E_{a\,j}(F)$.)

F_j / F_C	F_v / F_C	$\exists_a^{(0)}/\varepsilon$	γ /R	DW	$\langle \Delta r_{jv} \rangle$ /R	$F_{jv} / \varepsilon R^{-1}$	$\Delta U_{jv} / \varepsilon$
5	35	0.963	0.671	0.0572	0.671	0.474	0.955
5	65	0.902	0.541	0.0155	0.543	0.830	0.871
5	95	0.812	0.415	0.00707	0.417	1.19	0.744
35	65	0.749	0.414	0.0568	0.414	1.19	0.741
35	95	0.600	0.289	0.0154	0.289	1.55	0.570
65	95	0.362	0.164	0.0568	0.165	1.91	0.354

Table 8: Results from analysis of the force dependence of the activation energy for a dissociation process following a U_{PP} potential energy curve, (n = 2, s = 3.5 and q = 0.8) or (n = 3.5, s = 2 and q = 0.2), $F_C = 2.19\varepsilon R^{-1}$. (If $n_i = s_j$ and $n_j = s_i$ and $q_i = 1-q_j$, then $E_{a\,i}(F) = E_{a\,j}(F)$.)

F_j / F_C	F_v / F_C	$\exists_a^{(0)}/\varepsilon$	γ/R	DW	$\langle\Delta r_{jv}\rangle/R$	$F_{jv}/\varepsilon R^{-1}$	$\Delta U_{jv}/\varepsilon$
5	35	0.962	0.737	0.0573	0.738	0.432	0.953
5	65	0.899	0.591	0.0155	0.593	0.755	0.868
5	95	0.808	0.452	0.00709	0.455	1.08	0.741
35	65	0.742	0.449	0.0569	0.449	1.09	0.734
35	95	0.594	0.313	0.0154	0.313	1.42	0.564
65	95	0.357	0.177	0.0568	0.177	1.75	0.349

Table 9: Results from analysis of the force dependence of the activation energy for a dissociation process following a U_{PP} potential energy curve, (n = 11, s = 3.5 and q = 0.8) or (n = 3.5, s = 11 and q = 0.2), $F_C = 7.7\varepsilon R^{-1}$. (If $n_i = s_j$ and $n_j = s_i$ and $q_i = 1-q_j$, then $E_{a\,i}(F) = E_{a\,j}(F)$.)

F_j / F_C	F_v / F_C	$\exists_a^{(0)}/\varepsilon$	γ/R	DW	$\langle\Delta r_{jv}\rangle/R$	$F_{jv}/\varepsilon R^{-1}$	$\Delta U_{jv}/\varepsilon$
5	35	0.885	0.220	0.0615	0.224	1.41	0.873
5	65	0.791	0.157	0.0175	0.164	2.38	0.761
5	95	0.690	0.112	0.00822	0.121	3.34	0.640
35	65	0.584	0.103	0.0573	0.104	3.81	0.578
35	95	0.450	0.0679	0.0157	0.069	4.86	0.431
65	95	0.248	0.0352	0.0570	0.035	6.13	0.244

Table 10: Results from analysis of the force dependence of the activation energy for a dissociation process following a U_{PP} potential energy curve, (n = 11, s = 2 and q = 0.8) or (n = 2, s = 11 and q = 0.2), $F_C = 5.79\varepsilon R^{-1}$. (If $n_i = s_j$ and $n_j = s_i$ and $q_i = 1-q_j$, then $E_{a\,i}(F) = E_{a\,j}(F)$.)

F_j / F_C	F_v / F_C	$\exists_a^{(0)}/\varepsilon$	γ/R	DW	$\langle\Delta r_{jv}\rangle/R$	$F_{jv}/\varepsilon R^{-1}$	$\Delta U_{jv}/\varepsilon$
5	35	0.923	0.283	0.0602	0.286	1.08	0.913
5	65	0.846	0.216	0.0166	0.220	1.88	0.817
5	95	0.752	0.161	0.00761	0.166	2.69	0.694
35	65	0.669	0.154	0.0570	0.155	2.88	0.662
35	95	0.528	0.105	0.0155	0.106	3.72	0.503
65	95	0.308	0.0579	0.0569	0.0581	4.62	0.302

Table 11: Results from analysis of the force dependence of the activation energy for a dissociation process following a U_{PP} potential energy curve, (n = 3.5, s = 2 and q = 0.8) or (n = 2, s = 3.5 and q = 0.2), $F_C = 3.04\varepsilon R^{-1}$. (If $n_i = s_j$ and $n_j = s_i$ and $q_i = 1-q_j$, then $E_{a\,i}(F) = E_{a\,j}(F)$.)

F_j / F_C	F_v / F_C	$\exists_a^{(0)}/\varepsilon$	γ/R	DW	$\langle\Delta r_{jv}\rangle/R$	$F_{jv}/\varepsilon R^{-1}$	$\Delta U_{jv}/\varepsilon$
5	35	0.931	0.546	0.0590	0.551	0.577	0.921
5	65	0.853	0.415	0.0163	0.423	0.994	0.822
5	95	0.756	0.308	0.00750	0.319	1.41	0.697
35	65	0.671	0.295	0.0570	0.296	1.51	0.664
35	95	0.527	0.200	0.0155	0.203	1.95	0.503
65	95	0.305	0.109	0.0569	0.109	2.43	0.299

Table 12: Results from analysis of the force dependence of the activation energy for a dissociation process following a U_{PP} potential energy curve, (n = 3.5, s = 11 and q = 0.8) or (n = 11, s = 3.5 and q=0.2), $F_C = 4.05\varepsilon R^{-1}$. (If $n_i = s_j$ and $n_j = s_i$ and $q_i = 1-q_j$, then $E_{a\,i}(F) = E_{a\,j}(F)$.)

F_j / F_C	F_v / F_C	$\exists_a^{(0)}/\varepsilon$	γ/R	DW	$\langle\Delta r_{jv}\rangle/R$	$F_{jv}/\varepsilon R^{-1}$	$\Delta U_{jv}/\varepsilon$
5	35	0.912	0.417	0.0599	0.422	0.756	0.900
5	65	0.824	0.307	0.0168	0.316	1.29	0.793
5	95	0.724	0.223	0.00781	0.235	1.82	0.669
35	65	0.626	0.209	0.0572	0.210	2.01	0.620
35	95	0.486	0.139	0.0156	0.142	2.57	0.465
65	95	0.273	0.0734	0.0570	0.0739	3.23	0.268

Table 13: Results from analysis of the force dependence of the activation energy for a dissociation process following a U_{LJ} potential energy curve, $F_C = 2.396\varepsilon\sigma^{-1}$

F_j / F_C	F_v / F_C	$\exists_a^{(0)}/\varepsilon$	γ/R	DW	$\langle\Delta r_{jv}\rangle/R$	$F_{jv}/\varepsilon R^{-1}$	$\Delta U_{jv}/\varepsilon$
5	35	0.879	0.624	0.0648	0.637	0.416	0.871
5	65	0.808	0.473	0.0186	0.491	0.708	0.808
5	95	0.731	0.364	0.00860	0.385	1.03	0.731
35	65	0.655	0.344	0.0573	0.345	1.18	0.655
35	95	0.551	0.256	0.0157	0.259	1.56	0.551
65	95	0.390	0.173	0.0569	0.173	1.95	0.390

described with $U_{PP}(r)$, the underestimation of ε is more significant for dissociation pathways containing a transition or an associated state located on a potential-energy plateau, e.g. for large values of n if q is large, or for large values of s if q is small.

The values of the parameter γ obtained from the slopes of the line fits significantly underestimate the zero-force reaction-coordinate separation between the associated and the transition state, R: even more than the values of $\exists_a^{(0)}$ underestimate ε. For example, for a case

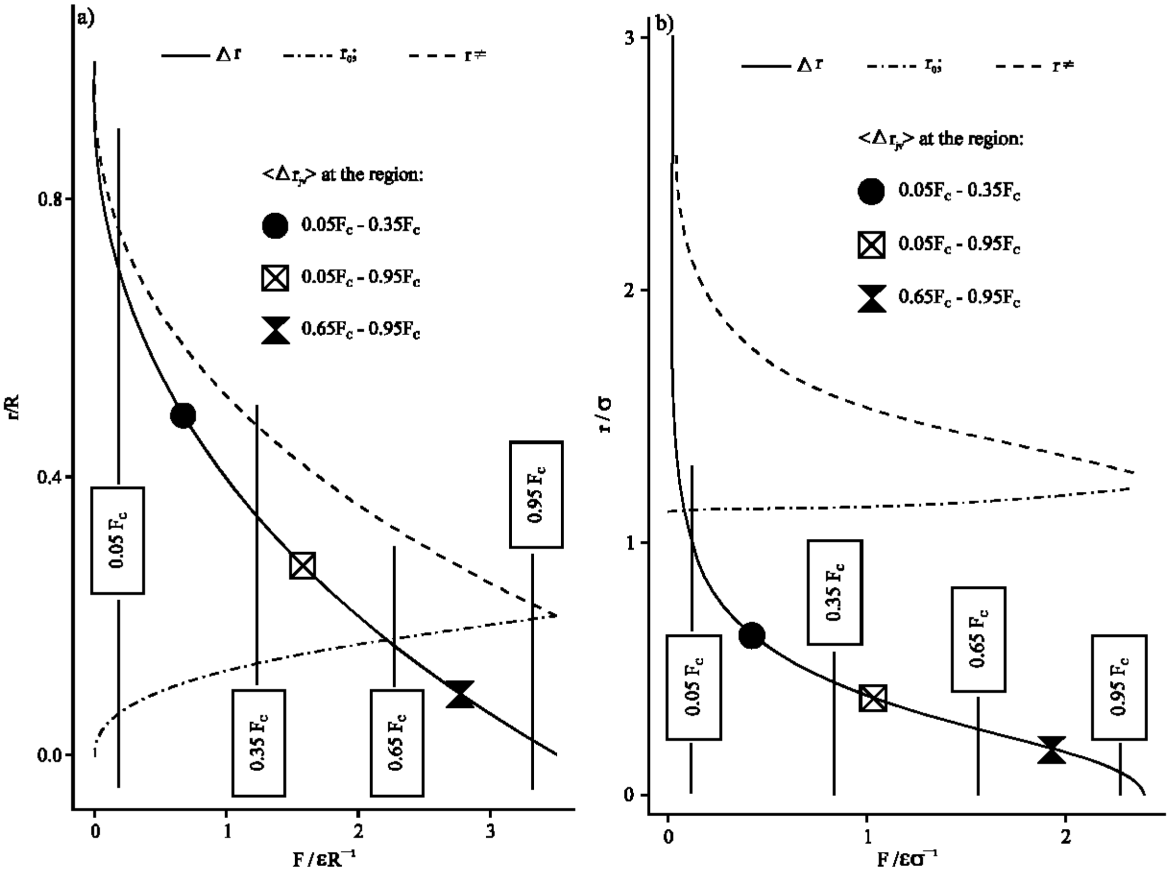

Fig. 6: Change in the positions of the associated and the transition state in the presence of external force for processes described by: (a) U_{PP} (q = 0.2; n = s = 3.5) and (b) U_{LJ}. Examples for the average values of Δr(F) obtained for three different force regions are placed on the curves (Eq. 17), between: $F_j = 0.05F_C$ and $F_v = 0.35F_C$; $F_j = 0.05F_C$ and $F_v = 0.95F_C$; $F_j = 0.35F_C$ and $F_v = 0.95F_C$.

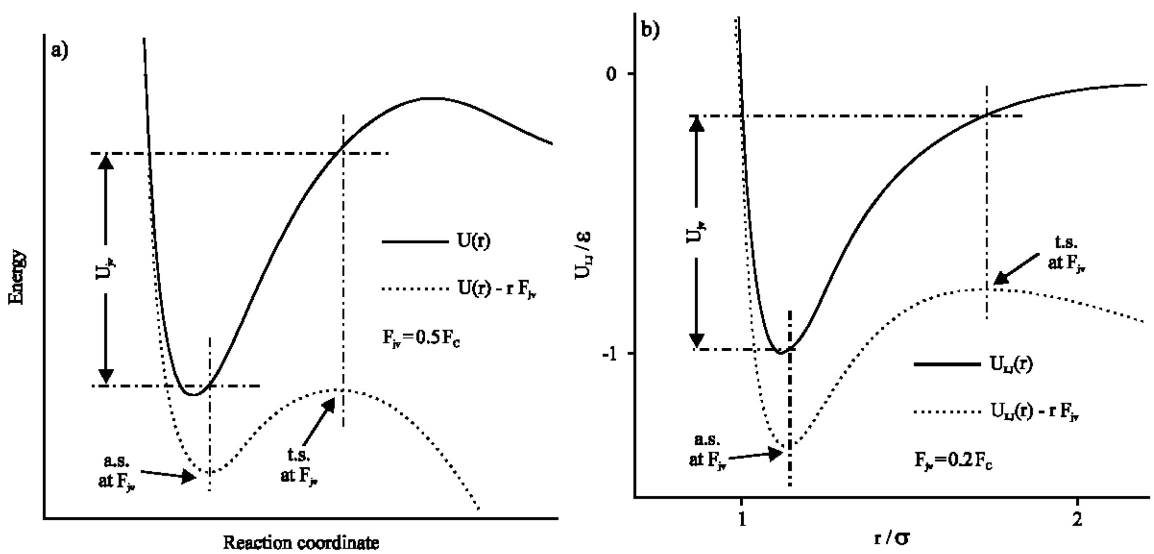

Fig. 7: Coordinate average energy, ΔU_{jv}, (Eq. 19) for a dissociation process with: (a) one transition state, $F_{jv} = 0.5F_C$ and (b) no transition state (U_{LJ}), $F_{jv} = 0.2F_C$

showing good activation-energy evaluation, i.e. $\ni_a^{(0)}/\varepsilon$ = 0.968, the value of γ is 0.8R (Table 1). Line fits, however, performed between $F_j = 0.65F_C$ and $F_v = 0.95F_C$, produce values for γ that are as much as ~ 45 times smaller than R (Table 2).

For all fitting regions between F_j and F_v, the force dependence of the reaction-coordinate separation between the associated and the transition state, $\Delta r(F)$, was examined and the force-average associated-transition state separations $<\Delta r_{jv}>$, calculated using Eq. (17b), are listed in Table 1 to 13 (Fig. 6). The values for F_{jv} were numerically determined (Eq. 18). Due to the lack of symmetry in the curvature of the $\Delta r(F)$ functions, the values of F_{jv} should not be identified with the average forces, $F_{jv} \neq |F_j-F_v| / 2$ (Fig. 6). Consequently, the values of F_{jv} are input in Eq. (19) for calculation of the coordinate-average energies, ΔU_{jv} (Fig. 7). The obtained average quantities, $<\Delta r_{jv}>$ and ΔU_{jv}, are listed in Table 1 to 13.

DISCUSSION

For the analysis of force-modulated kinetics, the potential energy function, U(r), which describes the unperturbed pathway of dissociation, is independent of the external force. Therefore, the solutions of Eq. 3 are force dependent, resulting in a nonlinear relationship between the activation energy of dissociation and the magnitude of the applied force. Furthermore, the plots of the activation energy vs. force (calculated with Eq. 4, 5 and 11b) have convex curvatures (Fig. 4): i.e. because U(r) is convex (i.e. $d^2U/dr^2 > 0$) at the associated state and concave (i.e. $d^2U/dr^2 < 0$) at the transition state, the resultant $E_a(F)$ will be a convex function. (Force independent solutions of Eq. 3 can be generated if $U(r) = F \int u(r)dr$, where, u(r) is a force independent function of r, making U(r) force dependent.)

Because of the linear relationship between the logarithmic value of the dissociation rate constant, $\ln(k_d(F))$ and the activation energy, $E_a(F)$, the shapes of the curves describing $E_a(F)$ and $\ln(k_d(F))$ are similar, i.e. $\ln(k_d(F)) \propto -E_a(F)$ and the results for $E_a(F)$ vs. F can be used for examination of the feasibility of Bell model. Due to the negative relationship, however, $\ln(k_d(F))$ is a concave function. Apparently, due to the convexity of $E_a(F)$ and concavity of $\ln(k_d(F))$, that is $d^2E_a(F)/dF^2 > 0$ and $d^2\ln(k_d(F))/dF^2 < 0$, analysis based on Bell model will result in underestimation of the zero-force activation energy, ε and overestimation of the zero-force rate constant of dissociation. Acceptable estimations of ε, however, can be achieved if the linear analyses are performed within a narrow range of relatively weak forces (Table 1 to 13).

The parameter γ is another important component of the Bell model (Eq. 1 and 2). The dimension of γ is reaction-coordinate length and it has been ascribed to the distance between the associated and the transition state in the reaction trajectory[4,6,24,32,33,38,41,43]. The results shown in Table 1-12, however, reveal that such an approximation, i.e. $\gamma \approx R$, is not truly satisfactory, especially if the associated or the transition state is located on a plateau of U(r), e.g. for large values of n if q is large or for large values of s if q is small.

If the dissociation process in the absence of external force does not proceed through a transition state, ascribing γ to $R = r^{*(0)}-r_0^{(0)}$ is, apparently, meaningless. For example, let the trajectory of interaction between two proteins follow Lennard-Jones shaped potential energy function and the half-depth width of the potential well of the associated state is about 0.2 nm, indicating that $\sigma \approx 0.6$ nm. The findings shown in Table 4 suggest that linear analysis of force-modulated kinetic data from such a system will yield $\gamma \approx 0.3$ to 0.4 nm, which is quite a reasonable value for the distance between the associated and the transition state for protein-ligand or protein-protein association/dissociation processes. Such an interpretation of γ is, obviously, misleading and does not reflect the characteristics of the examined system.

The resemblance between Eq. 1c and 5c suggests for a different interpretation of γ (and $\ni_a^{(0)}$). Eq. (1c and 17b), furthermore, suggest that symmetry in the concavity of the $E_a(F)$ curves in the fitting regions will result in identical values for γ and $<\Delta r_{jv}>$: i.e. if $(E_a(F_j) + \gamma F_j) \to (E_a(F_v) + \gamma F_v)$, then $\gamma \to <\Delta r_{jv}>$. Comparison of the values of $<\Delta r_{jv}>$ with the values of γ, listed in Table 1 to 13, shows an excellent correlation between the two quantities (Fig. 8a), with the tendency for γ to be slightly smaller or equal to $<\Delta r_{jv}>$. The latter discrepancy results from the lack of symmetry in the concavity of the $E_a(F)$ curves within the fitting force region.

Although the excellent correlation shown on Fig. 8a does not prove that γ and $<\Delta r_{jv}>$ have identical physical meanings, it demonstrates that application of the Bell model for analyses at different force ranges will produce a series of parameters γ that can be used for determination of the changes in the reaction-coordinate separation between the transition and the associated state when external force is applied. Furthermore, Eq. 1c, 5c and 6 indicate that narrowing the region of a linear fit, i.e. $\Delta F = F_v-F_j \to dF$, causes the value of γ to asymptotically approach the negative of the first force derivative of $E_a(F)$, which is, indeed, $\Delta r(F)$ (Eq. 6).

Taking the resemblance between Eq. 1c and 5c a step further can produce an alternative interpretation of

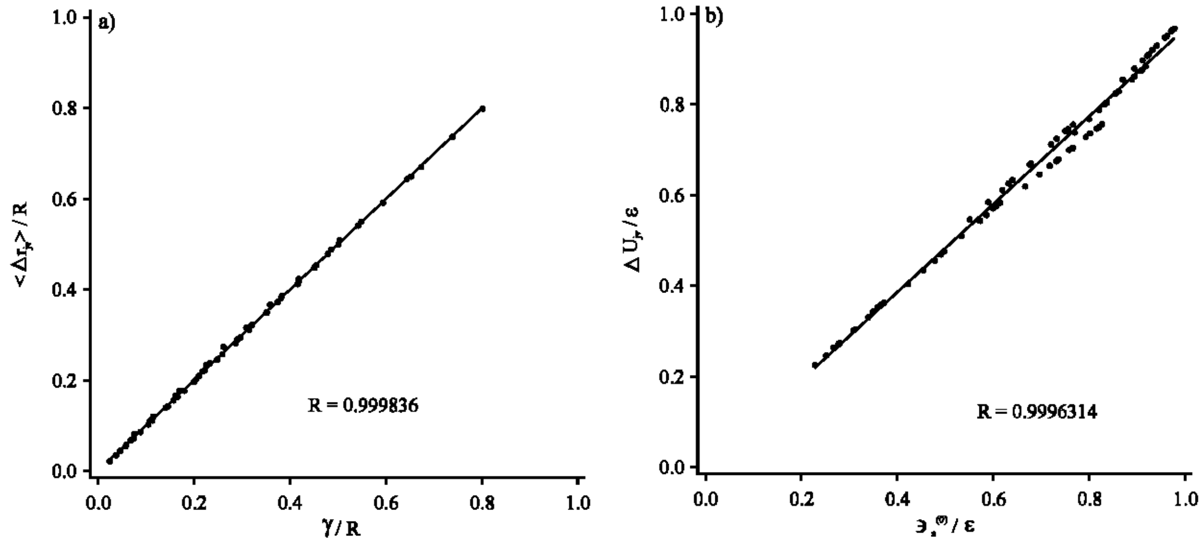

Fig. 8: Correlation analyses with the corresponding correlation coefficients, R, between: (a) parameter γ and the force-average associated-transition state separation, $<\Delta r_{jv}>$ and (b) the interceptions, $\ni_a^{(0)}$ and the coordinate-average energy, ΔU_{jv}, The black dots are points corresponding to values obtained from the 12 different $E_a(F)$ and $\Delta r(F)$ curves for dissociation processes described by U_{PP} (q = 0.2, 0.5, 0.8; n = 2, 3.5, 11 and s = 2, 3.5, 11) for six force intervals: 0.05-0.35, 0.05-0.65, 0.05-0.95, 0.35-0.65, 0.35-0.95 and 0.65-0.95F_C

the intercept, $\ni_a^{(0)}$. Table 1 to 13 show the calculated values of the coordinate-average energy, ΔU_{jv}, which reflects the potential-energy difference between points on the force-unperturbed U(r); these points have the reaction coordinates of the associated and the transition state at force F_{jv} (Eq. 5a). The values of ΔU_{jv}, apparently, correlate quite well with the corresponding intercepts from the line fits, $\ni_a^{(0)}$ (Fig. 8b).

Because of the correlation between $\ni_a^{(0)}$ and the coordinate-average energy, ΔU_{jv}, as well as between γ and the force-average associated-transition state separation $<\Delta r_{jv}>$ (Fig. 7), the Bell expression for linear analysis of force-modulated kinetics, $E_a(F)$ vs. F, can be rewritten as:

$$E_a(F)\Big|_{F_j}^{F_v} = = \Delta U_{jv} - <\Delta r_{jv}> F \qquad (20)$$

Data fitting at narrow ranges of weak forces, i.e. $|F_v-F_j| << F_C$ and $F_v << F_C$, will indeed allow for approximation of ΔU_{jv} to the zero-force activation energy, ε or $E_a^{(0)}$ and $<\Delta r_{jv}>$ to the zero-force separation between the associated and the transition state, R or $\Delta r^{(0)}$. Equation 20, however, further indicates that linear fits at different force regions will produce a series of values for $<\Delta r_{jv}>$ and ΔU_{jv}. The values for force-average associated-transition state separation can elucidate how the pulling force changes the reaction-coordinate separation between the transition and the associated state (Fig. 6), while the values of coordinate-average energy are equal to potential-energy differences at various coordinates along the reaction coordinates in the absence of external force (Fig. 7). Such set of data can prove quite useful for quantitative mapping of energy landscapes and trajectories of dissociation processes.

CONCLUSIONS

Application of an external pulling force (Schemes 1 and 2) causes a decrease in the activation energy of dissociation, E_a. Because the force dependence of the activation energy, $E_a(F)$, is described by a convex function (Fig. 4), intercepts, $\ni_a^{(0)}$, obtained from linear analysis of $E_a(F)$ vs. F, always underestimate the activation energy in absence of force (Table 1-13). Due to the negative linear relationship between the logarithm of the rate constant and activation energy, (Eq. 2), similar analysis of experimentally obtained dissociation rates will result in overestimation of the rate constants at zero force. Such overestimation of the rate constants and underestimation of the activation energies can be minimized if the linear analysis is limited to forces much smaller than the critical force. For example, for a representative enzyme-ligand system (R = $\Delta r^{(0)}$ ~ 0.5 nm; ε = $E_a^{(0)}$ ~ 10 kcal mol^{-1}; n = s = 2), 20% of F_C is about 55 pN; hence, application of the Bell model for measurements collected between 5 and 55 pN will estimate $\ln(k_d^{(0)})$ and/or $E_a^{(0)}$ within 5% of their real values. Application of such forces is within the aptitude of numerous techniques for single-molecule force measurements.

The values of the parameters γ obtained from the slopes of the linear fits based on the Bell-model analysis, Eq. (1 and 2), deviate significantly from the reaction-coordinate separation, $\Delta r^{(0)}$, between the transition and the associated state in the unperturbed system. (The superscript (0) designates quantities in the absence of external force, i.e. at $F = 0$.) In addition, such distance, $\Delta r^{(0)}$, is meaningless for dissociation processes that do not proceed through transition states at zero force.

The coordinate-average energies, ΔU_{jv}, obtained at different force regions, are related to different values of $<\Delta r_{jv}>$ that can range from 0 to R (Fig. 7). Therefore, a spectrum of ΔU_{jv} vs. $<\Delta r_{jv}>$ will be informative about the shape of the reaction trajectory between the associated and the transition state and can be utilized for mapping the potential-energy profiles of dissociation pathways.

The presented analysis is based on general expressions (Eq. 3-7) that do not impose any limitations on the shape of the reaction trajectory, therefore, the conclusions are valid for any dissociation process that proceeds through no more than one transition state.

ACKNOWLEDGMENT

My gratitude is extended to the U.S. Army Research Laboratory for their support for this research.

REFERENCES

1. Ratcliff, G.C. and D.A. Erie, 2001. A novel single-molecule study to determine protein-protein association constants. J. Am. Chem. Soc., 123: 5632-5635.
2. Zhang, X., E. Wojcikiewicz and V.T. Moy, 2002. Force spectroscopy of the leukocyte function-associated antigen-1/intercellular adhesion molecule-1 interaction. Biophys. J., 83: 2270-2279.
3. Kokkoli, E., S.E. Ochsenhirt and M. Tirrell, 2004. Collective and single-molecule interactions of a5b1 integrins. Langmuir, 20: 2397-2404.
4. Kuehner, F., L.T. Costa, P.M. Bisch, S. Thalhammer, W.M. Heckl and H.E. Gaub, 2004. LexA-DNA bond strength by single molecule force spectroscopy. Biophys. J., 87: 2683-2690.
5. Baumgartner, W., P. Hinterdorfer, W. Ness, A. Raab, D. Vestweber, H. Schindler and D. Drenckhahn, 2000. Cadherin interaction probed by atomic force microscopy. Proc. Natl. Acad. Sci. USA., 97: 4005-4010.
6. Meadows, P.Y., J.E. Bemis and G.C. Walker, 2003. Single-molecule force spectroscopy of isolated and aggregated fibronectin proteins on negatively charged surfaces in aqueous liquids. Langmuir, 19: 9566-9572.
7. Engel, A. and M. Hegner, 2004. Atomic force microscopy and laser tweezers. Schriften des Forschungszentrums Juelich, Reihe Materie und Material, 19: B4/1-B4/16.
8. Leckband, D., 2000. Measuring the forces that control protein interactions. Ann. Rev. Biophys. Biomol. Str., 29: 1-26.
9. Dudko, O.K., A.E. Filippov, J. Klafter and M. Urbakh, 2003. Beyond the conventional description of dynamic force spectroscopy of adhesion bonds. Proc. Natl. Acad. Sci. USA., 100: 11378-11381.
10. Merkel, R., P. Nassoy, A. Leung, K. Ritchie and E. Evans, 1999. Energy landscapes of receptor-ligand bonds explored with dynamic force spectroscopy. Nature, 397: 50-53.
11. Friedsam, C., A.K. Wehle, F. Kuehner and H.E. Gaub, 2003. Dynamic single-molecule force spectroscopy: Bond rupture analysis with variable spacer length. J. Phys. Condensed Matter, 15: S1709-S1723.
12. Pierres, A., D. Touchard, A.M. Benoliel and P. Bongrand, 2002. Dissecting streptavidin-biotin interaction with a laminar flow chamber. Biophys. J., 82: 3214-3223.
13. Thomas, W.E., E. Trintchina, M. Forero, V. Vogel and E.V. Sokurenko, 2002. Bacterial adhesion to target cells enhanced by shear force. Cell, 109: 913-923.
14. Kuo, S.C., 2001. Using optics to measure biological forces and mechanics. Traffic, 2: 757-763.
15. Mehta, A.D., M. Rief, J.A. Spudich, D.A. Smith and R.M. Simmons, 1999. Single-molecule biomechanics with optical methods. Science, 283: 1689-1698.
16. Lister, I., R. Roberts, S. Schmitz, M. Walker, J. Trinick, C. Veigel, F. Buss and J. Kendrick-Jones, 2004. Myosin VI: A multifunctional motor. Biochem. Soc. Transactions, 32: 685-688.
17. Danilowicz, C., D. Greenfield and M. Prentiss, 2005. Dissociation of ligand-receptor complexes using magnetic tweezers. Anal. Chem., 77: 3023-3028.
18. Abels, J.A., F. Moreno-Herrero, T. Van der Heijden, C. Dekker and N.H. Dekker, 2005. Single-molecule measurements of the persistence length of double-stranded RNA. Biophys. J., 88: 2737-2744.
19. Danilowicz, C., V.W. Coljee, C. Bouzigues, D.K. Lubensky, D.R. Nelson and M. Prentiss, 2003. DNA unzipped under a constant force exhibits multiple metastable intermediates. Proc. Natl. Acad. Sci. USA, 100: 1694-1699.
20. Assi, F., R. Jenks, J. Yang, C. Love and M. Prentiss, 2002. Massively parallel adhesion and reactivity measurements using simple and inexpensive magnetic tweezers. J. Applied Phys., 92: 5584-5586.

21. Guttenberg, Z., A.R. Bausch, B. Hu, R. Bruinsma, L. Moroder and E. Sackmann, 2000. Measuring ligand-receptor unbinding forces with magnetic beads: molecular leverage. Langmuir, 16: 8984-8993.
22. Saleh, O.A., C. Perals, F.X. Barre and J.F. Allemand, 2004. Fast, DNA-sequence independent translocation by FtsK in a single-molecule experiment. EMBO J., 23: 2430-2439.
23. Janshoff, A., M. Neitzert, Y. Oberdorfer and H. Fuchs, 2000. Force spectroscopy of molecular systems-single molecule spectroscopy of polymers and biomolecules. Angewandte Chemie, International Edition, 39: 3212-3237.
24. Evstigneev, M. and P. Reimann, 2003. Dynamic force spectroscopy: optimized data analysis. Physical Review E: Statistical, Nonlinear and Soft Matter Physics, 68: 045103/045101-045103/045104.
25. Dietz, H. and M. Rief, 2004. Exploring the energy landscape of GFP by single-molecule mechanical experiments. Proc. Natl. Acad. Sci. United States of America, 101: 16192-16197.
26. Heymann, B. and H. Grubmuller, 2000. Dynamic Force Spectroscopy of Molecular Adhesion Bonds. Phys. Rev. Lett., 84: 6126-6129.
27. Bongrand, P., 1999. Ligand-receptor interactions. Reports on Progress in Physics, 62: 921-968.
28. Evans, E., 2001. Probing the relation between force--lifetime--and chemistry in single molecular bonds. Ann. Rev. Biophys. Biomol. Str., 30: 105-128.
29. Bell, G.I., 1978. Models for the specific adhesion of cells to cells. Science, 200: 618-627.
30. de Chateau, M., S. Chen, A. Salas and T.A. Springer, 2001. Kinetic and Mechanical Basis of Rolling through an Integrin and Novel Ca^{2+}-Dependent Rolling and Mg^{2+}-Dependent Firm Adhesion Modalities for the a4b7-MAdCAM-1 Interaction. Biochemistry, 40: 13972-13979.
31. Erdmann, T. and U.S. Schwarz, 2004. Stochastic dynamics of adhesion clusters under shared constant force and with rebinding. J. Chem. Phys., 121: 8997-9017.
32. Strunz, T., K. Oroszlan, I. Schumakovitch, H.J. Guntherodt and M. Hegner, 2000. Model energy landscapes and the force-induced dissociation of ligand-receptor bonds. Biophys. J., 79: 1206-1212.
33. Noy, A., S. Zepeda, C.A. Orme, Y. Yeh and J.J. De Yoreo, 2003. Entropic barriers in nanoscale adhesion studied by variable temperature chemical force microscopy. J. Am. Chem. Soc., 125: 1356-1362.
34. Galligan, E., C.J. Roberts, M.C. Davies, S.J.B. Tendler and P. M. Williams, 2001. Simulating the dynamic strength of molecular interactions. J. Chem. Phys., 114: 3208-3214.
35. Haenggi, P., P. Talkner and M. Borkovec, 1990. Reaction-rate theory: fifty years after Kramers. Rev. Modern Phys., 62: 251-341.
36. Evans, E. and K. Ritchie, 1999. Strength of a weak bond connecting flexible polymer chains. Biophys. J., 76: 2439-2447.
37. Evans, E., 1998. Energy landscapes of biomolecular adhesion and receptor anchoring at interfaces explored with dynamic force spectroscopy. Faraday discussion, pp: 1-16.
38. Hummer, G. and A. Szabo, 2003. Kinetics from nonequilibrium single-molecule pulling experiments. Biophys. J., 85: 5-15.
39. Evans, E. and K. Ritchie, 1997. Dynamic strength of molecular adhesion bonds. Biophys. J., 72: 1541-1555.
40. Auletta, T., M.R. De Jong, A. Mulder, F.C.J.M. Van Veggel, J. Huskens, D.N. Reinhoudt, S. Zou, S. Zapotoczny, H. Schoenherr, G.J. Vancso and L. Kuipers, 2004. b-Cyclodextrin host-guest complexes probed under thermodynamic equilibrium: thermodynamics and AFM force spectroscopy. J. Am. Chem. Soc., 126: 1577-1584.
41. Bustanji, Y., C.R. Arciola, M. Conti, E. Mandello, L. Montanaro and B. Samori, 2003. Dynamics of the interaction between a fibronectin molecule and a living bacterium under mechanical force. Proc. Natl. Acad. Sci. United States of America, 100: 13292-13297.
42. Strigl, M., D.A. Simson, C.M. Kacher and R. Merkel, 1999. Force-induced dissociation of single protein A-IgG bonds. Langmuir, 15: 7316-7324.
43. Zhang, X., S.E. Craig, H. Kirby, M.J. Humphries and V.T. Moy, 2004. Molecular basis for the dynamic strength of the integrin a4b1/VCAM-1 interaction. Biophys. J., 87: 3470-3478.
44. Pellicane, G., D. Costa and C. Caccamo, 2004. Theory and simulation of short-range models of globular protein solutions. Los Alamos National Laboratory, Preprint Archive, Condensed Matter, pp: 1-17, arXiv:cond-mat/0407335.
45. Clementi, E., G. Ranghino and R. Scordamaglia, 1977. Intermolecular potentials: Interaction of water with lysozyme. Chem. Phy. Lett., 49: 218-224.
46. Stewart, K.D., J.A. Bentley and M. Cory, 1990. DOCKing ligands into receptors: The test case of a-chymotrypsin. Tetrahedron Computer Methodol., 3: 713-722.
47. ten Wolde, P.R. and D. Frenkel, 1997. Enhancement of protein crystal nucleation by critical density fluctuations. Science, 277: 1975-1978.
48. Rutledge, D.N. and A.S. Barros, 2002. Durbin-Watson statistic as a morphological estimator of information content. Analytica Chimica Acta, 454: 277-295.
49. Eaton, D.F., 1990. Recommended methods for fluorescence decay analysis. Pure Applied Chem., 62: 1631-1648.